Exploiting noncircularity in backscattering communications

Donatella Darsena

Dipartimento di Ingegneria
Università Parthenope, Napoli, Italy,
Email: darsena@uniparthenope.it

Giacinto Gelli and Francesco Verde

Dipartimento di Ingegneria Elettrica e delle Tecnologie dell'Informazione
Università Federico II, Napoli, Italy,
Email: [gelli, f.verde]@unina.it

***Abstract*—In backscatter radio systems, a passive (i.e., battery-free) device (so-called tag) is able to transmit information by harvesting energy from a carrier transmitted by an access point or base station (so-called reader), thus enabling significant power savings compared to traditional wireless communication schemes. In this paper, the physical layer of a backscatter system is revisited to develop a design framework encompassing the use of multiple antennas at both the reader and the tag, as well as the exploitation of symbol noncircularity through the employment of a widely-linear equalizer at the reader. It is also outlined how the choice of noncircular multilevel modulation formats can be coupled with optimized power harvesting at the tag.**

I. Introduction

In recent years, with the proliferation of small communication-enabled objects and the emergence of the Internet-of-Things (IoT) paradigm, research on *backscattering communications (BCs)* has been receiving an increasing attention. Different from traditional communication techniques, BCs enable small devices to communicate by modulating the reflection of an incident (EM) electromagnetic field. Significant applications of BCs are in radio frequency identification (RFID) systems, where the information stored in a lightweight device (the *tag*) is read by illuminating it with a continuous-wave signal emitted by a close device (the *reader*), which is able to decode the backscattered signal. RFID systems operating in the ultra high frequency (UHF) band have been recently standardized [1]. Other applications of BCs are in the field of so called "ambient backscattering" [2], [3], where two devices can communicate using ambient radio-frequency (RF) signals, such as, e.g., those emitted by television systems [2] or wireless local area networks [3].

The design of BC systems [4] involves interesting tradeoffs between power efficiency [i.e., the ability of the device to harvest direct current (DC) energy from the impinging RF signal], reliability (in terms of symbol error probability), data-rate, coverage, and complexity. In BC devices, the circuit input impedance is switched between a matched state (where the device maximizes energy harvesting) and a number of deliberate mismatched states, which introduce amplitude and/or phase modulation in the reflected wave. Existing RFID standards [1] allows one to employ simple binary modulations, such as binary amplitude-shift keying (BASK) or binary phase-shift keying (BPSK). However, several studies consider the extension of BCs to higher-order modulations, such as quadrature-amplitude modulation (QAM), typically 4-QAM or 16-QAM [5], [6], allowing one to improve the data-rate performance. In [6], in particular, the design of the BC system is carried out by jointly taking into account the link reliability and the loss of power harvesting capability due to backscattering modulation: in the case of maximum likelihood (ML) detection and 4-QAM modulation, it is shown that optimal constellations are not square, but rectangular ones and, hence, they are non circular [7]. In [8], [9] the introduction of multiple antennas at the reader and tag is explored as a means of improving communication reliability by *pinhole* diversity: indeed, the backscattering link can be modeled as a *dyadic backscatter channel* (DBC), a particular *keyhole* or *pinhole* channel [10], where the pinholes are the tag antennas [9].

In this paper, focusing on UHF RFID-like systems, we consider the design of a BC system employing multiple antennas at the reader and the tag, and exploiting the noncircular properties [7] of the symbol constellations. Unlike previous works [5], [6], symbol noncircularity is explicitly accounted for in order to equalize the considered multiple-input multiple-output (MIMO) DBC by means of widely-linear (WL) minimum mean-square error (MMSE) filtering [11]. A multilevel constellation constrained optimization design is additionally proposed that ensures noncircularity of the transmitted symbol and improved power harvesting functionalities for the tag.

II. Signal model of a backscatter radio system

In a MIMO BCs system (Fig. 1) the reader is equipped with N_{T} transmit and N_{R} receive antennas, whereas the passive tag employs N_{B} antennas. The ith reader antenna transmits an unmodulated continuous waveform (CW) having amplitude $c_i > 0$, angular frequency ω_{c}, and phase $\psi_i \in [0, 2\,\pi)$, with $1 \leq i \leq N_{\mathrm{T}}$: such CW signals impinges on tag antennas and are partly scattered back.

For $1 \leq i \leq N_{\mathrm{T}}$, $1 \leq p \leq N_{\mathrm{B}}$, and $1 \leq n \leq N_{\mathrm{R}}$, the

This work was partially supported by the "Centro Regionale Information Communication Technology" (CeRICT).

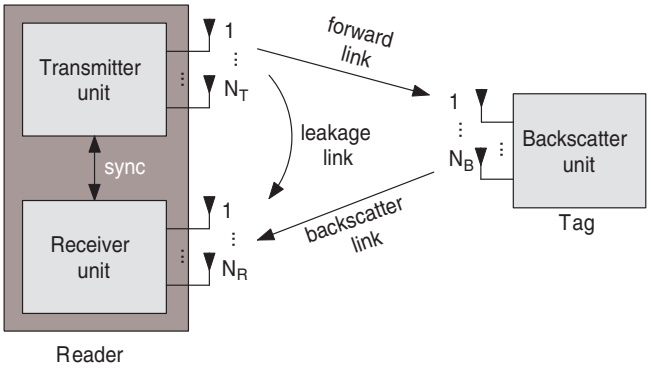

Figure 1. Block diagram of a MIMO backscatter radio system with N_{T} transmitter antennas, N_{R} receiver antennas, and N_{B} backscatter antennas.

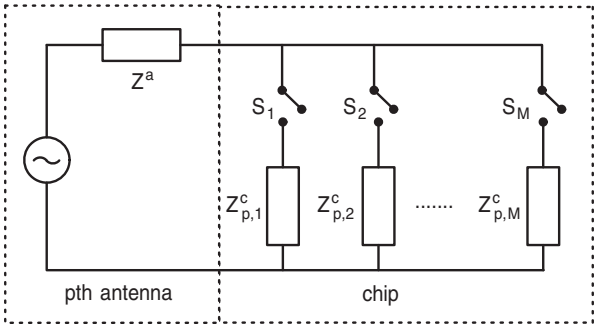

Figure 2. Equivalent circuit of a multilevel passive backscattering device.

channels corresponding to the $i \to p$ reader-to-tag (*forward*) link and to the $p \to n$ tag-to-reader (*backscatter*) link are assumed to be frequency-flat and quasi-stationary: they are modeled by the complex coefficients f_{pi} and b_{np}, respectively, which are constant within one transmission (e.g., one reading of the tag), but are allowed to vary from transmission to transmission. In the following subsections, we describe in detail the signal models at the tag and at the reader.[1]

A. Backscattered signal by the passive tag

According to the antenna scatterer theorem [12], the EM field backscattered from an antenna is divided [12] into load-dependent (or *antenna mode*) scattering and load-independent (or *structural mode*) one: the former component can be associated with re-radiated power and depends on the load impedance, whereas the latter one can be interpreted as scattering from an open-circuited antenna.

In a BC system, the tag acts as a digital multilevel modulator, mapping each information symbol onto a set of M waveforms by means of a proper variation of its chip impedance [5]. To elaborate upon this point, Fig. 2 reports the equivalent Thévenin circuit [13] of the pth ($1 \le p \le N_{\mathrm{B}}$) antenna tag front-end, where the sine wave generator models the sinusoidal voltage induced by the reader's incident EM field, $Z^{\mathrm{a}} = R^{\mathrm{a}} + j\,X^{\mathrm{a}} \in \mathbb{C}$ is the antenna impedance,[2] and $Z^{\mathrm{c}}_{p,m} = R^{\mathrm{c}}_{p,m} + j\,X^{\mathrm{c}}_{p,m} \in \mathbb{C}$ ($1 \le m \le M$) are M distinct values of the pth tag chip impedance, which determines the antenna mode component of the backscattered field.

With reference to antenna mode scattering, a generic sample of the symbol-spaced baseband-equivalent signal backscattered by the pth tag antenna can be expressed as

$$x_p = G_p \sum_{i=1}^{N_{\mathrm{T}}} f_{pi}\, c_i\, e^{j\psi_i} \tag{1}$$

where $G_p \in \mathbb{C}$ is the power wave reflection coefficient [14], whose squared magnitude $|G_p|^2 \le 1$ measures the fraction of the maximum power available from the generator (see Fig. 2) that is not delivered to the tag chip.[3] When the switch S_m is closed, i.e., the chip impedance of the tag front-end is given by $Z^{\mathrm{c}}_{p,m}$, the coefficient G_p assumes [14] the value

$$\Gamma_{p,m} \triangleq \frac{(Z^{\mathrm{a}})^* - Z^{\mathrm{c}}_{p,m}}{Z^{\mathrm{a}} + Z^{\mathrm{c}}_{p,m}}\,. \tag{2}$$

It is worth noticing that, if $(Z^{\mathrm{a}})^* = Z^{\mathrm{c}}_{p,m}$ (*impedance matching condition*), then $\Gamma_{p,m} = 0$: in this case, the tag achieves maximum average power harvesting. Let $\mathcal{P}_{\max}$ denote the average power harvested under the impedance matching condition, when the switch S_m is closed, the power $\mathcal{P}^{\mathrm{h}}_p$ harvested by the pth tag antenna during backscatter takes on the value $\Pi_{p,m} \triangleq \mathcal{P}_{\max}(1 - |\Gamma_{p,m}|^2)$.

The backscattered signal x_p in (1) is a scalar multiple of G_p, whose values, given by (2), are determined by the tag chip impedance $Z^{\mathrm{c}}_{p,m}$. Therefore, a multilevel digital modulation can be realized for each tag antenna by mapping the information symbols into the set $\mathcal{G}_p \triangleq \{\Gamma_{p,1}, \Gamma_{p,2}, \ldots, \Gamma_{p,M}\}$ of reflection coefficients. Such a mapping is also referred to as *backscatter or load modulation*.

For $1 \le p \le N_{\mathrm{B}}$, let $a_p \in \mathbb{C}$ denote the symbol to be transmitted by the pth antenna of the tag, which assumes equiprobable values in the set $\mathcal{A} \triangleq \{\alpha_1, \alpha_2, \ldots, \alpha_M\}$;[4] the following linear mapping between G_p and a_p is typically considered (see, e.g., [5]):

$$G_p = \eta\, a_p \tag{3}$$

[1] The fields of complex and real numbers are denoted with $\mathbb{C}$ and $\mathbb{R}$, respectively; matrices [vectors] are denoted with upper [lower] case boldface letters (e.g., $\mathbf{A}$ or $\mathbf{a}$); the field of $m \times n$ complex [real] matrices is denoted as $\mathbb{C}^{m\times n}$ [$\mathbb{R}^{m\times n}$], with $\mathbb{C}^m$ [$\mathbb{R}^m$] used as a shorthand for $\mathbb{C}^{m\times 1}$ [$\mathbb{R}^{m\times 1}$]; the superscripts $*$, T, H, and -1 denote the conjugate, the transpose, the conjugate transpose, and the inverse of a matrix, respectively; if $\mathbf{A} \in \mathbb{C}^{n\times n}$ is nonsingular, $\mathbf{A}^{-*}$ stands for $(\mathbf{A}^*)^{-1}$; $\Re\{a\}$ and $\Im\{a\}$ are the real and imaginary part of $a \in \mathbb{C}$, respectively; the magnitude and phase of $a \in \mathbb{C}$ are denoted with $|a|$ and $\angle a$, respectively; for any $\mathbf{a} \in \mathbb{C}^n$, $\|\mathbf{a}\|$ denotes the Euclidean norm; $\mathrm{rank}(\mathbf{A})$, $\det(\mathbf{A})$, and $\mathrm{tr}(\mathbf{A})$ denote the rank, the determinant, and the trace of $\mathbf{A} \in \mathbb{C}^{n\times n}$; $\mathbf{O}_{m\times n} \in \mathbb{R}^{m\times n}$ and $\mathbf{I}_m \in \mathbb{R}^{m\times m}$ denote the null and the identity matrices, respectively; matrix $\mathbf{A} = \mathrm{diag}(a_0, a_1, \ldots, a_{n-1}) \in \mathbb{C}^{n\times n}$ is diagonal; $\{\mathbf{A}\}_{i_1 i_2}$ indicates the (i_1, i_2)th element of $\mathbf{A} \in \mathbb{C}^{n\times m}$; $j \triangleq \sqrt{-1}$ is the imaginary unit and the operator $\mathbb{E}[\,\cdot\,]$ denotes ensemble averaging.

[2] We assume that all tag antennas are characterized by the same impedance.

[3] The reflection coefficient depends on the chip impedance that, in its turn, depends on the chip input power. This dependence causes the reflection coefficient to be nonlinear. A linearized model is assumed for the tag's reflection coefficient [15], where G_p does not depend on the incident power.

[4] It is assumed that symbols transmitted by different tag antennas are drawn from the same signal constellation.

with $\eta \in \mathbb{R}$. As a consequence, the power wave reflection coefficient G_p and the harvested power $\mathcal{P}_p^{\mathrm{h}}$ can be modeled as (discrete) random variables assuming equiprobable values in the sets $\mathcal{G}_p$ and $\mathcal{P}_p \triangleq \{\Pi_{p,1}, \Pi_{p,2}, \ldots, \Pi_{p,M}\}$, respectively.

Both η and the symbol constellation $\mathcal{A}$ of a_p values in (3) must be carefully designed. To fulfil the physical constraint $|\Gamma_{p,m}| \leq 1$, it is imposed that $0 < \eta \leq 1$ and the symbol constellation is normalized such as $|\alpha_m| \leq 1$ for each element of $\mathcal{A}$. Moreover, the choice of η governs the harvesting-performance tradeoff. Indeed, values of η closer to 1 allows the tag to reflect increasing amounts of the incident field back to the reader, resulting thus in greater backscatter signal strengths, i.e., for a target symbol error probability (SEP) at the reader, larger communication ranges. On the other hand, values of η much smaller than 1 allow a larger part of the incident field to be absorbed by the RF-to-DC conversion circuits of the tag, hence improving power conversion at the expense of backscatter signal strength.

Once η and $\mathcal{A}$ are chosen in accordance with certain criteria and, thus, the set $\mathcal{G}$ is identified through (3), the impedance set $\mathcal{Z}_p^{\mathrm{c}} \triangleq \{Z_{p,1}^{\mathrm{c}}, Z_{p,2}^{\mathrm{c}}, \ldots, Z_{p,M}^{\mathrm{c}}\}$ corresponding to the designed signal constellation can be obtained from (2) as follows

$$Z_{p,m}^{\mathrm{c}} = \frac{(Z^{\mathrm{a}})^* - Z^{\mathrm{a}}\,\Gamma_{p,m}}{1 + \Gamma_{p,m}} \tag{4}$$

where the antenna impedance Z^{a} is given. It is noteworthy that, since the impedance $Z_{p,m}^{\mathrm{c}}$ is physically realizable if its resistive component is non-negative, i.e., $\Re(Z_{p,m}^{\mathrm{c}}) \geq 0$, the symbol constellation has to be designed by also taking into account the following constraint

$$\Re\left[\frac{(Z^{\mathrm{a}})^* - Z^{\mathrm{a}}\,\Gamma_{p,m}}{1 + \Gamma_{p,m}}\right] \geq 0\,. \tag{5}$$

Other constraints may arise when calculating $Z_{p,m}^{\mathrm{c}}$ using (4): for instance, to reduce the physical size of the tag, it might be required to use resistors and capacitors, by eliminating inductive components [5]. In the sequel, for the sake of mathematical tractability, we will consider constraint (5) only.

B. Received signal at the reader

A snapshot of the symbol-spaced baseband-equivalent signal received at the nth receive antenna can be written as

$$y_n = \sum_{p=1}^{N_{\mathrm{B}}} b_{np}\, x_p + d_n + v_n \tag{6}$$

for $1 \leq n \leq N_{\mathrm{R}}$, where $d_n \triangleq s_n + \ell_n$ accounts for both the structural mode scattering $s_n \in \mathbb{C}$, which is independent of the tag chip impedances, as well as the leakage ℓ_n from the reader's transmit unit (see Fig. 1), whereas $v_n \in \mathbb{C}$ is thermal noise. Specifically, the antenna leakage term can be decomposed as $\ell_n = \sum_{i=1}^{N_{\mathrm{T}}} h_{ni}\, c_i\, e^{j\psi_i}$, where h_{ni} the complex channel coefficient between the ith transmit antenna and the nth receiver antenna of the reader.

By defining the vector $\mathbf{y} \triangleq [y_1, y_2, \ldots, y_{N_{\mathrm{R}}}]^{\mathrm{T}} \in \mathbb{C}^{N_{\mathrm{R}}}$ and taking int account (6), one obtains the following compact vector model of the received signal

$$\mathbf{y} = \mathbf{B}\,\mathbf{G}\,\mathbf{F}\,\mathbf{c} + \mathbf{d} + \mathbf{v} \tag{7}$$

where $\mathbf{B} \in \mathbb{C}^{N_{\mathrm{R}} \times N_{\mathrm{B}}}$ and $\mathbf{F} \in \mathbb{C}^{N_{\mathrm{B}} \times N_{\mathrm{T}}}$ collect the channel coefficients of the backscatter and forward links, respectively, i.e., $\{\mathbf{B}\}_{np} \triangleq b_{np}$ and $\{\mathbf{F}\}_{pi} \triangleq f_{pi}$, with $1 \leq i \leq N_{\mathrm{T}}$, $1 \leq p \leq N_{\mathrm{B}}$, and $1 \leq n \leq N_{\mathrm{R}}$, the matrix $\mathbf{G} \triangleq \mathrm{diag}(G_1, G_2, \ldots, G_{N_{\mathrm{B}}}) \in \mathbb{C}^{N_{\mathrm{B}} \times N_{\mathrm{B}}}$ gathers the reflection coefficients, which are linked to the symbols transmitted by the tag through (3) and therefore represent the desired information to be estimated at the reader, the vector $\mathbf{c} \triangleq [c_1\, e^{j\psi_1}, c_2\, e^{j\psi_2}, \ldots, c_{N_{\mathrm{T}}}\, e^{j\psi_{N_{\mathrm{T}}}}]^{\mathrm{T}} \in \mathbb{C}^{N_{\mathrm{T}}}$ is *known* at the reader, $\mathbf{d} \triangleq [d_1, d_2, \ldots, d_{N_{\mathrm{R}}}]^{\mathrm{T}} \in \mathbb{C}^{N_{\mathrm{R}}}$, and $\mathbf{v} \triangleq [v_1, v_2, \ldots, v_{N_{\mathrm{R}}}]^{\mathrm{T}} \in \mathbb{C}^{N_{\mathrm{R}}}$. Additionally, it results that $\mathbf{d} = \mathbf{s} + \boldsymbol{\ell}$, where $\mathbf{s} \triangleq [s_1, s_2, \ldots, s_{N_{\mathrm{R}}}]^{\mathrm{T}} \in \mathbb{C}^{N_{\mathrm{R}}}$ and $\boldsymbol{\ell} \triangleq [\ell_1, \ell_2, \ldots, \ell_{N_{\mathrm{R}}}]^{\mathrm{T}} = \mathbf{H}\,\mathbf{c} \in \mathbb{C}^{N_{\mathrm{R}}}$, with $\{\mathbf{H}\}_{ni} \triangleq h_{ni}$.

The signal model (7) defines a $N_{\mathrm{T}} \times N_{\mathrm{B}} \times N_{\mathrm{R}}$ DBC [8], [9]. According to such a model, signal propagation in a MIMO backscatter radio system is described by means of a pinhole channel. In the context of MIMO active wireless transceivers, a pinhole channel is a MIMO link whose capacity is equivalent to that of a single-input single-output link operating at the same signal-to-noise ratio (SNR) as that of the MIMO link [10]. In [9] it is shown that, in the BC channel, space-time coding techniques allows one to exploit pinhole diversity, whose asymptotic order is N_{B}.

III. Widely-linear equalization of a DBC

The main task of the reader is to reliably estimate from (7) the symbol block $\mathbf{a} \triangleq [a_1, a_2, \ldots, a_{N_{\mathrm{B}}}]^{\mathrm{T}} \in \mathbb{C}^{N_{\mathrm{B}}}$ transmitted by the tag, whose elements are embedded in the diagonal entries of $\mathbf{G}$. With moderate or large number of antennas, the ML receiver implemented with Viterbi's algorithm might have unaffordable complexity. This motivates looking for less computationally expensive equalizing strucures as linear ones. If the received vector $\mathbf{y}$ is noncircular (or improper) [7] (see Section IV), WL equalizing structures [11] generalize and outperform linear ones. Herein, we will focus on the WL-MMSE criterion because it offers almost perfect symbol recovery in high SNR regimes and its performance is easily computable with accurate approximations. Thanks to its reduced complexity, the WL-MMSE equalizer may be used in practice to successfully equalize DBCs.

To derive from (7) the mathematical structure of the WL-MMSE equalizer, accounting for (3), it is mathematically convenient to rewrite $\mathbf{y}$ as follows

$$\mathbf{y} = \eta\,\mathbf{B}\,\boldsymbol{\Sigma}\,\mathbf{a} + \mathbf{d} + \mathbf{v} = \eta\,\boldsymbol{\Psi}\,\mathbf{a} + \mathbf{d} + \mathbf{v} \tag{8}$$

where $\boldsymbol{\Sigma} \triangleq \mathrm{diag}(\mathbf{f}_1^{\mathrm{T}}\mathbf{c}, \mathbf{f}_2^{\mathrm{T}}\mathbf{c}, \ldots, \mathbf{f}_{N_{\mathrm{B}}}^{\mathrm{T}}\mathbf{c}) \in \mathbb{C}^{N_{\mathrm{B}} \times N_{\mathrm{B}}}$, with $\mathbf{f}_p^{\mathrm{T}}$ denoting the pth row of $\mathbf{F}$, and $\boldsymbol{\Psi} \triangleq \mathbf{B}\,\boldsymbol{\Sigma} \in \mathbb{C}^{N_{\mathrm{R}} \times N_{\mathrm{B}}}$ collects parameters that are known at the reader. The forthcoming derivations of the WL-MMSE equalizer are based on the following three assumptions:

(a1) the "composite" matrix $\boldsymbol{\Psi}$, as well as the "structured" disturbance (i.e., structural mode scattering plus reader-to-reader leakage) vector $\mathbf{d}$, are known at the reader;

(a2) the symbol vector $\mathbf{a}$ transmitted by the tag is zero-mean and has correlation matrix $\mathbf{R}_{\mathbf{aa}} \triangleq \mathbb{E}[\mathbf{a}\,\mathbf{a}^{\mathrm{H}}] = \sigma_a^2\,\mathbf{I}_{N_{\mathrm{B}}}$, with $\sigma_a^2 \triangleq \mathbb{E}[|a_p|^2] > 0$, and conjugate correlation matrix $\mathbf{R}_{\mathbf{aa}^*} \triangleq \mathbb{E}[\mathbf{a}\,\mathbf{a}^{\mathrm{T}}] = \rho_a\,\mathbf{I}_{N_{\mathrm{B}}}$, with $\rho_a \triangleq \mathbb{E}[a_p^2] \in \mathbb{C}$;

(a3) the noise vector $\mathbf{v}$ is zero-mean, with correlation matrix $\mathbf{R}_{\mathbf{vv}} \triangleq \mathbb{E}[\mathbf{v}\,\mathbf{v}^{\mathrm{H}}] = \sigma_v^2\,\mathbf{I}_{N_{\mathrm{R}}}$ and conjugate correlation matrix $\mathbf{R}_{\mathbf{vv}^*} \triangleq \mathbb{E}[\mathbf{v}\,\mathbf{v}^{\mathrm{T}}] = \mathbf{O}_{N_{\mathrm{R}}\times N_{\mathrm{R}}}$; moreover, $\mathbf{v}$ is statistically independent of $\mathbf{a}$.

Assumption **(a1)** is reasonable since $\mathbf{\Psi}$ and $\mathbf{s}$ can be estimated at the reader using training symbols transmitted by the tag, whereas the reader can alone estimate $\boldsymbol{\ell} = \mathbf{H}\,\mathbf{c}$ during the silent periods of the tag. Assumption **(a2)** essentially states that the tag implements a MIMO scheme with *spatial multiplexing*, i.e., it transmits independent symbols over different antennas. Moreover, on the basis of assumption **(a2)**, the pth symbol $a_p = \Re(a_p) + j\,\Im(a_p)$ transmitted by the tag is noncircular (or improper) [7] if

$$\rho_a = \mathbb{E}[\Re^2(a_p)] - \mathbb{E}[\Im^2(a_p)] + 2\,j\,\mathbb{E}[\Re(a_p)\,\Im(a_p)] \neq 0\,. \quad (9)$$

It is important to observe that, since $|\alpha_m| \leq 1$ for each element of $\mathcal{A}$, then $\sigma_a^2 \leq 1$. Moreover, by invoking the Cauchy-Schwartz inequality, it results that $|\rho_a| \leq \sigma_a^2$. We will show in Section IV that condition (9) is fulfilled when the constellation design jointly accounts for equalization performance at the reader and power harvesting at the tag. Finally, the fact that $\mathbf{R}_{\mathbf{vv}^*} = \mathbf{O}_{N_{\mathrm{R}}\times N_{\mathrm{R}}}$ in assumption **(a3)** implies that the noise vector is circular (or proper) [16].

Since $\mathbf{d}$ is known at the reader [see assumption **(a1)**], we can consider the vector $\mathbf{r} \triangleq \mathbf{y} - \mathbf{d} = \eta\,\mathbf{\Psi}\,\mathbf{a} + \mathbf{v}$ [see (8)]. The input-output relationship of a WL equalizer [11] reads as

$$\mathbf{z} = \mathbf{W}_1\,\mathbf{r} + \mathbf{W}_2\,\mathbf{r}^* = \mathbf{W}\,\tilde{\mathbf{r}} \quad (10)$$

where $\mathbf{W}_1 \in \mathbb{C}^{N_{\mathrm{B}}\times N_{\mathrm{R}}}$ and $\mathbf{W}_2 \in \mathbb{C}^{N_{\mathrm{B}}\times N_{\mathrm{R}}}$ are *filtering matrices*, $\mathbf{W} \triangleq [\mathbf{W}_1, \mathbf{W}_2] \in \mathbb{C}^{N_{\mathrm{B}}\times 2N_{\mathrm{R}}}$, and $\tilde{\mathbf{r}} \triangleq [\mathbf{r}^{\mathrm{T}}, \mathbf{r}^{\mathrm{H}}]^{\mathrm{T}} \in \mathbb{C}^{2N_{\mathrm{R}}}$. From the expression of $\mathbf{r}$, the *augmented* vector $\tilde{\mathbf{r}}$ is given by

$$\tilde{\mathbf{r}} = \eta\,\tilde{\mathbf{\Psi}}\,\tilde{\mathbf{a}} + \tilde{\mathbf{v}} \quad (11)$$

where

$$\tilde{\mathbf{\Psi}} \triangleq \begin{bmatrix} \mathbf{\Psi} & \mathbf{O}_{N_{\mathrm{R}}\times N_{\mathrm{B}}} \\ \mathbf{O}_{N_{\mathrm{R}}\times N_{\mathrm{B}}} & \mathbf{\Psi}^* \end{bmatrix} \in \mathbb{C}^{2N_{\mathrm{R}}\times 2N_{\mathrm{B}}} \quad (12)$$

$\tilde{\mathbf{a}} \triangleq [\mathbf{a}^{\mathrm{T}}, \mathbf{a}^{\mathrm{H}}]^{\mathrm{T}} \in \mathbb{C}^{2N_{\mathrm{B}}}$ and $\tilde{\mathbf{v}} \triangleq [\mathbf{v}^{\mathrm{T}}, \mathbf{v}^{\mathrm{H}}]^{\mathrm{T}} \in \mathbb{C}^{2N_{\mathrm{R}}}$. In accordance with assumption **(a2)**, the correlation matrix of $\tilde{\mathbf{a}}$ can be expressed as

$$\mathbf{R}_{\tilde{\mathbf{a}}\tilde{\mathbf{a}}} \triangleq \mathbb{E}[\tilde{\mathbf{a}}\,\tilde{\mathbf{a}}^{\mathrm{H}}] = \begin{bmatrix} \sigma_a^2\,\mathbf{I}_{N_{\mathrm{B}}} & \rho_a\,\mathbf{I}_{N_{\mathrm{B}}} \\ \rho_a^*\,\mathbf{I}_{N_{\mathrm{B}}} & \sigma_a^2\,\mathbf{I}_{N_{\mathrm{B}}} \end{bmatrix} \in \mathbb{C}^{2N_{\mathrm{B}}\times 2N_{\mathrm{B}}}\,. \quad (13)$$

By using the formula for the determinant of block-wise partitioned matrices, one has $\det(\mathbf{R}_{\tilde{\mathbf{a}}\tilde{\mathbf{a}}}) = (\sigma_a^4 - |\rho_a|^2)^{N_{\mathrm{B}}} \geq 0$, which shows that $\mathbf{R}_{\tilde{\mathbf{a}}\tilde{\mathbf{a}}}$ is rank deficient if and only if (iff) $|\rho_a| = \sigma_a^2$, i.e., there exists a *mean-square* linear dependence between a_p and its conjugate a_p^*.[5] Moreover, from assumption **(a3)**, one has $\mathbf{R}_{\tilde{\mathbf{v}}\tilde{\mathbf{v}}} \triangleq \mathbb{E}[\tilde{\mathbf{v}}\,\tilde{\mathbf{v}}^{\mathrm{H}}] = \sigma_v^2\,\mathbf{I}_{2N_{\mathrm{R}}}$.

[5]Such a linear dependence is exhibited by real symbol sequences and complex modulation formats with offset [17].

The WL-MMSE criterion amounts to minimizing (with respect to $\mathbf{W}$) the mean square error $\mathrm{MSE}(\mathbf{W}) \triangleq \mathbb{E}[\|\mathbf{z}-\mathbf{a}\|^2]$. If we introduce the following change of variables

$$\mathbf{W} \rightarrow \tilde{\mathbf{W}} \triangleq \begin{bmatrix} \mathbf{W}_1 & \mathbf{W}_2 \\ \mathbf{W}_2^* & \mathbf{W}_1^* \end{bmatrix} \in \mathbb{C}^{2N_{\mathrm{B}}\times 2N_{\mathrm{R}}} \quad (14)$$

it is verified that $2\,\mathrm{MSE}(\mathbf{W}) = \tilde{\mathrm{MSE}}(\tilde{\mathbf{W}}) \triangleq \mathbb{E}[\|\tilde{\mathbf{z}} - \tilde{\mathbf{a}}\|^2]$, where $\tilde{\mathbf{z}} \triangleq [\mathbf{z}^{\mathrm{T}}, \mathbf{z}^{\mathrm{H}}]^{\mathrm{T}} = \tilde{\mathbf{W}}\,\tilde{\mathbf{r}}$ [see eq. (10)]. Consequently, the optimal matrix $\mathbf{W}_{\mathrm{opt}} \triangleq [\mathbf{W}_{1,\mathrm{opt}}, \mathbf{W}_{2,\mathrm{opt}}]$, with $\mathbf{W}_{1,\mathrm{opt}} \in \mathbb{C}^{N_{\mathrm{B}}\times N_{\mathrm{R}}}$ and $\mathbf{W}_{2,\mathrm{opt}} \in \mathbb{C}^{N_{\mathrm{B}}\times N_{\mathrm{R}}}$, minimizes $\mathrm{MSE}(\mathbf{W})$ iff

$$\tilde{\mathbf{W}}_{\mathrm{opt}} \triangleq \begin{bmatrix} \mathbf{W}_{1,\mathrm{opt}} & \mathbf{W}_{2,\mathrm{opt}} \\ \mathbf{W}_{2,\mathrm{opt}}^* & \mathbf{W}_{1,\mathrm{opt}}^* \end{bmatrix} \quad (15)$$

minimizes $\tilde{\mathrm{MSE}}(\tilde{\mathbf{W}})$. Solution $\tilde{\mathbf{W}}_{\mathrm{opt}}$ can be found by setting to zero the complex gradient of $\tilde{\mathrm{MSE}}(\tilde{\mathbf{W}})$ with respect to $\tilde{\mathbf{W}}$, thus obtaining $\tilde{\mathbf{W}}_{\mathrm{opt}} = \eta\,\mathbf{R}_{\tilde{\mathbf{a}}\tilde{\mathbf{a}}}\,\tilde{\mathbf{\Psi}}^{\mathrm{H}}(\eta^2\,\tilde{\mathbf{\Psi}}\,\mathbf{R}_{\tilde{\mathbf{a}}\tilde{\mathbf{a}}}\,\tilde{\mathbf{\Psi}}^{\mathrm{H}} + \sigma_v^2\,\mathbf{I}_{2N_{\mathrm{R}}})^{-1}$, from which, by using the formula for the inverse of block-wise partitioned matrices, one gets

$$\mathbf{W}_{1,\mathrm{opt}} = \eta\,(\sigma_a^2\,\mathbf{\Psi}^{\mathrm{H}} - \rho_a\,\mathbf{\Psi}^{\mathrm{T}}\,\mathbf{R}_{\mathbf{rr}}^{-*}\,\mathbf{R}_{\mathbf{rr}^*}^*)\,(\mathbf{R}_{\mathbf{rr}}/\mathbf{R}_{\tilde{\mathbf{r}}\tilde{\mathbf{r}}})^{-*} \quad (16)$$

$$\mathbf{W}_{2,\mathrm{opt}} = \eta\,(\rho_a\,\mathbf{\Psi}^{\mathrm{T}} - \sigma_a^2\,\mathbf{\Psi}^{\mathrm{H}}\,\mathbf{R}_{\mathbf{rr}}^{-1}\,\mathbf{R}_{\mathbf{rr}^*})\,(\mathbf{R}_{\mathbf{rr}}/\mathbf{R}_{\tilde{\mathbf{r}}\tilde{\mathbf{r}}})^{-1} \quad (17)$$

where $\mathbf{R}_{\mathbf{rr}}/\mathbf{R}_{\tilde{\mathbf{r}}\tilde{\mathbf{r}}} \triangleq \mathbf{R}_{\mathbf{rr}}^* - \mathbf{R}_{\mathbf{rr}^*}^*\,\mathbf{R}_{\mathbf{rr}}^{-1}\,\mathbf{R}_{\mathbf{rr}^*} \in \mathbb{C}^{N_{\mathrm{R}}\times N_{\mathrm{R}}}$ is the Schur complement of $\mathbf{R}_{\mathbf{rr}}$ in $\mathbf{R}_{\tilde{\mathbf{r}}\tilde{\mathbf{r}}} \triangleq \mathbb{E}[\tilde{\mathbf{r}}\,\tilde{\mathbf{r}}^{\mathrm{H}}] \in \mathbb{C}^{2N_{\mathrm{R}}\times 2N_{\mathrm{R}}}$ and, according to assumptions **(a2)** and **(a3)**, it results that $\mathbf{R}_{\mathbf{rr}} \triangleq \mathbb{E}[\mathbf{r}\,\mathbf{r}^{\mathrm{H}}] = \eta^2\,\sigma_a^2\,\mathbf{\Psi}\,\mathbf{\Psi}^{\mathrm{H}} + \sigma_v^2\,\mathbf{I}_{N_{\mathrm{R}}}$ and $\mathbf{R}_{\mathbf{rr}^*} \triangleq \mathbb{E}[\mathbf{r}\,\mathbf{r}^{\mathrm{T}}] = \eta^2\,\rho_a\,\mathbf{\Psi}\,\mathbf{\Psi}^{\mathrm{T}}$. As it is expected, when the symbols are circular [16], i.e., $\rho_a = 0$, it follows that $\mathbf{W}_{1,\mathrm{opt}} = \mathbf{L}_{\mathrm{opt}} \triangleq \eta\,\sigma_a^2\,\mathbf{\Psi}^{\mathrm{H}}\,\mathbf{R}_{\mathbf{rr}}^{-1}$ and $\mathbf{W}_{2,\mathrm{opt}} = \mathbf{O}_{N_{\mathrm{B}}\times N_{\mathrm{R}}}$, i.e., the WL-MMSE equalizer ends up to its linear counterpart.

The *error-performance surface* of the WL-MMSE equalizer is given by $\mathrm{MSE}_{\mathrm{WL}}(\eta, |\rho_a|) \triangleq \mathrm{MSE}(\mathbf{W}_{\mathrm{opt}}) = \tilde{\mathrm{MSE}}(\tilde{\mathbf{W}}_{\mathrm{opt}})/2$ and it can be expressed as

$$\begin{aligned}\mathrm{MSE}_{\mathrm{WL}}(\eta, |\rho_a|) &= \sigma_a^2\,N_{\mathrm{B}} - \frac{\eta}{2}\,\mathrm{tr}(\tilde{\mathbf{W}}_{\mathrm{opt}}\,\tilde{\mathbf{\Psi}}\,\mathbf{R}_{\tilde{\mathbf{a}}\tilde{\mathbf{a}}}) \\ &= \sigma_a^2\,N_{\mathrm{B}} - \eta\,\sigma_a^2\,\mathrm{tr}(\mathbf{W}_{1,\mathrm{opt}}\,\mathbf{\Psi}) - \eta\,\rho_a^*\,\mathrm{tr}(\mathbf{W}_{2,\mathrm{opt}}\,\mathbf{\Psi}^*)\,. \quad (18)\end{aligned}$$

By substituting the expression of $\mathbf{R}_{\mathbf{rr}^*}$ in (18) ($\mathbf{R}_{\mathbf{rr}}$ does not depend on ρ_a), it can be verified that the MSE of the equalizer (16)-(17) does not depend on the phase of ρ_a. Moreover, we observe that the error-performance surface of the L-MMSE equalizer is obtained by setting $\rho_a = 0$ in (18), thus yielding

$$\mathrm{MSE}_{\mathrm{L}}(\eta) \triangleq \mathrm{MSE}_{\mathrm{WL}}(\eta, 0) = \sigma_a^2\,N_{\mathrm{B}} - \eta\,\sigma_a^2\,\mathrm{tr}(\mathbf{L}_{\mathrm{opt}}\,\mathbf{\Psi})\,. \quad (19)$$

On the other hand, when the magnitude of ρ_a takes on its maximum value, i.e., $|\rho_a| = \sigma_a^2$, it is readily checked that $\mathbf{W}_{2,\mathrm{opt}} = e^{j\angle\rho_a}\,\mathbf{W}_{1,\mathrm{opt}}^*$ and, thus, one obtains

$$\mathrm{MSE}_{\mathrm{WL}}(\eta, \sigma_a^2) = \sigma_a^2\,N_{\mathrm{B}} - 2\,\eta\,\sigma_a^2\,\mathrm{tr}(\mathbf{W}_{1,\mathrm{opt}}\,\mathbf{\Psi})\,. \quad (20)$$

At this point, we are in the position of studying the behavior of the performance difference between the WL-MMSE equalizer $\mathbf{W}_{\mathrm{opt}}$ and its linear counterpart $\mathbf{L}_{\mathrm{opt}}$. To this end, we report in Fig. 3 the ratio between the MSE performances of the L-MMSE and WL-MMSE equalizers, i.e., $\Lambda(\eta, |\rho_a|) \triangleq \mathrm{MSE}_{\mathrm{L}}(\eta)/\mathrm{MSE}_{\mathrm{WL}}(\eta, |\rho_a|)$, as a function of η (governing the backscatter signal strength) and $|\rho_a|$ (measuring

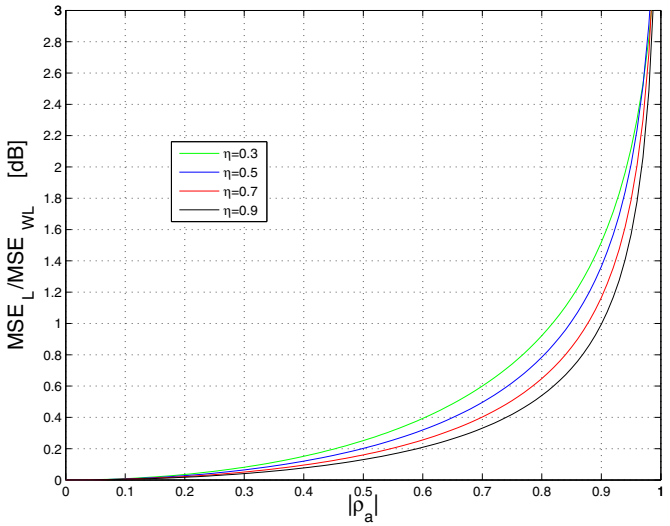

Figure 3. $\Lambda(\eta, |\rho_a|)$ versus $|\rho_a|$ for different values of η.

the degree of noncircularity of the tag symbols). Such curves are obtained by considering a Rayleigh fading scenario, i.e., the entries of $\mathbf{B}$ and $\mathbf{F}$ are independent and identically distributed (i.i.d.) zero-mean unit-variance circularly symmetric complex Gaussian random variables. The ensemble average of $\Lambda(\eta, |\rho_a|)$ with respect to $\mathbf{B}$ and $\mathbf{F}$ are evaluated through 10^3 Monte Carlo trials, by setting $(N_{\mathrm{T}}, N_{\mathrm{B}}, N_{\mathrm{R}}) = (2, 2, 2)$, $\mathbf{c} = [1, \ldots, 1]^{\mathrm{T}}/\sqrt{N_{\mathrm{T}}}$, $\sigma_a^2 = 1$, and SNR $\triangleq \sigma_a^2/\sigma_v^2 = 20$ dB.

It is seen from Fig. 3 that, for a given value of η, the performance gain of the WL-MMSE equalizer over the L-MMSE one is an increasing function of $|\rho_a|$, i.e., of the degree of noncircularity of the symbol transmitted by the tag; in particular, significant performance gains can be achieved for $|\rho_a| \to \sigma_a^2$: in this case, $\Lambda(\eta, |\rho_a|)$ tends to its maximum value given by the ratio between (19) and (20). On the other hand, for a given value of ρ_a, increasing values of η reduce the advantage of using a WL equalizer since they lead to greater backscatter signal strengths or, equivalently, higher SNR values;[6] however, when $\eta \to 1$, the RF power harvested by the tag tends to be vanishingly small. Hence, WL equalizers are particularly suited for passive backscattering radio systems.

IV. Noncircular constellation design

In passive BC systems, the power level harvested by the tag has to be sufficiently large to allow a reliable communication with the reader. A global measure of the energy harvested (per symbol) by the tag is the following one (see [6])

$$\mathbb{E}[\mathcal{P}_p^{\mathrm{h}}] = \frac{1}{M}\sum_{m=1}^{M} \Pi_{p,m} = \frac{\mathcal{P}_{\max}}{M}\sum_{m=1}^{M}(1 - \eta^2 |\alpha_m|^2) \qquad (21)$$

where we have also used (3). Assuming a fixed constellation size M, the set $\mathcal{A}$ can be chosen by maximizing (21) subject to the constraints: **(c1)** $\mathrm{MSE}_{\mathrm{WL}}(\eta, |\rho_a|) \leq \gamma_{\mathrm{th}}$, where $\gamma_{\mathrm{th}} > 0$ is a given threshold; **(c2)** the symbols transmitted by the tag are noncircular; **(c3)** inequality (5) is fulfilled for $1 \leq m \leq M$.

According to constraint **(c1)**, let $\overline{\eta}$ and $|\overline{\rho}_a|$ belong to the the subset of $(0, 1] \times [0, \sigma_a^2]$ characterized by the inequality $\mathrm{MSE}_{\mathrm{WL}}(\eta, |\rho_a|) \leq \gamma_{\mathrm{th}}$, constraint **(c2)** reads as

$$\frac{1}{M}\left|\sum_{m=1}^{M} \alpha_m^2\right| = |\overline{\rho}_a| \,. \qquad (22)$$

Using (3) and assuming $\Re\{Z^{\mathrm{a}}\} = R^{\mathrm{a}} \geq 0$, after some straightforward algebraic manipulations, constraint **(c3)** amounts to

$$\overline{\eta}^2 |\alpha_m|^2 - 1 \leq 0 \quad \text{for each } 1 \leq m \leq M \,. \qquad (23)$$

Therefore, the proposed optimization problem boils down to

$$\min_{\alpha_1, \alpha_2, \ldots, \alpha_M} \sum_{m=1}^{M} |\alpha_m|^2 \quad \text{subject to (22) and (23)} \qquad (24)$$

which is non-convex and a local solution can be found by means of numerical algorithms (details are omitted).

[6] Provided that $\mathbf{\Psi}$ is full-column rank, WL processing does not improve upon conventional linear processing in the high-SNR region [18].

References

[1] EPCglobal, "EPC radio-frequency identify protocols Class-1 Generation-2 UHF RFID", available on http://www.epcglobalinc.org.

[2] V. Liu, A. Parks, V. Talla, S. Gollakota, D. Wetherall, and J.R. Smith, "Ambient backscatter: wireless communication out of thin air", in *Proc. of ACM SIGCOMM'13*, Hong Kong, China, Aug. 2013, pp. 39–50.

[3] B. Kellogg, A. Parks, S. Gollakota, J.R. Smith, and D. Wetherall, "Wi-Fi backscatter: Internet connectivity for RF-powered devices", in *Proc. of ACM SIGCOMM'14*, Chicago, Illinois, USA, Aug. 2014, pp. 607–618.

[4] C. Boyer and S. Roy, "Backscatter communication and RFID: Coding, Energy, and MIMO analysis", *IEEE Trans. Commun.*, pp. 770–785, Mar. 2014.

[5] S.J. Thomas, E. Wheeler, J. Teizer, and M.S. Reynolds, "Quadrature amplitude modulated backscatter in passive and semipassive UHF RFID systems", *IEEE Trans. Microw. Theory Tech.*, pp. 1175–1182, Apr. 2012.

[6] C. Boyer and S. Roy, "Coded QAM backscatter modulation for RFID", *IEEE Trans. Commun.*, pp. 1925–1934, July 2012.

[7] P.J. Schreier and L.L. Scharf, "Second-order analysis of improper complex random vectors and processes", *IEEE Trans. Signal Process.*, pp. 714–725, Mar. 2003.

[8] J.D. Griffin and G.D. Durgin, "Gains for RF tags using multiple antennas", *IEEE Trans. Antennas Propag.*, pp. 563–570, Feb. 2008.

[9] C. Boyer and S. Roy, "Space time coding for backscatter RFID", *IEEE Trans. Wireless Commun.*, pp. 2272 –2280, May 2013.

[10] D. Gesbert, H. Bölcskei, D.A. Gore, and A.J. Paulraj, "Outdoor MIMO Wireless Channels: Models and Performance Prediction", *IEEE Trans. Commun.*, pp. 1926–1934, Dec. 2002.

[11] B. Picinbono and P. Chevalier, "Widely linear estimation with complex data", *IEEE Trans. Signal Process.*, pp. 2030–2033, Aug. 1995.

[12] R.C. Hansen,"Relationships between antennas as scatters and radiators", *Proc. IEEE*, pp. 659–662, May 1969.

[13] D.D. King,"The measurement and interpretation of antenna scattering", *Proc. IRE*, pp. 770–777, July 1949.

[14] K. Kurokawa, "Power waves and the scattering matrix", *IEEE Trans. Microw. Theory Tech.*, pp. 194–202, Mar. 1965.

[15] D. Arnitz, U. Muehlmann, and K. Witrisal, "Tag-based sensing and positioning in passive UHF RFID: Tag reflection", in *Proc. of 3rd Int. EURASIP Workshop RFID Technol.*, Cartagena, Spain, Sep. 2010, pp. 51–56.

[16] B. Picinbono, "On circularity", *IEEE Trans. Signal Process.*, pp. 3473–3482, Dec. 1994.

[17] D. Darsena, G. Gelli, L. Paura and F. Verde, "Subspace-based blind channel identification of SISO-FIR systems with improper random inputs", *Eurasip Journal on Signal Processing, Special Issue on Signal Processing in Communications*, pp. 2021–2039, Nov. 2004.

[18] A. S. Cacciapuoti, G. Gelli, L. Paura, and F. Verde, "Finite-sample performance analysis of widely-linear multiuser receivers in DS-CDMA systems," *IEEE Trans. Signal Process.*, pp. 1572–1588, Apr. 2008.